25th ABCM International Congress of Mechanical Engineering
October 20-25, 2019, Uberlândia, MG, Brazil

COB-2019-0904
CONTROL OF A MAGNETIC LEVITATION SYSTEM USING GLOVER-MCFARLANE H_∞ LOOP SHAPING DESIGN

Caio Igor Gonçalves Chinelato
Instituto Federal de São Paulo – IFSP – Campus São Paulo, R. Pedro Vicente, 625, Canindé, 01109-010, São Paulo, SP, Brasil
caio.chinelato@ifsp.edu.br

Abstract. *This work describes the control design and implementation for a magnetic levitation system. The system is composed by a Y shape iron plate that must be levitated by the control of electromagnetic forces. The system is nonlinear, open loop unstable and multivariable, whose inputs are represented by voltages applied to three electromagnets and the outputs are represented by three plate positions. A controller must be designed so that the plate positions track input references with adequate performance. The proposed method to control the system uses Glover-McFarlane H_∞ loop shaping design. This method is a combination of H_∞ robust stabilization with classical loop shaping and presents good performance and robustness when applied to several control problems. For the evaluation of controller, numerical simulations results were obtained with Matlab/Simulink. The numerical simulation results indicate that the controller presents stability, good performance and robustness.*

Keywords: *Magnetic Levitation System, H_∞ Design, Glover-McFarlane H_∞ Loop Shaping, Robust Control, Multivariable Control.*

1. INTRODUCTION

Magnetic levitation (maglev) systems have practical importance in many engineering systems such as in magnetic bearings, high precision positioning platform, aerospace shuttles, and fast maglev trains (Choudhary et al, 2012). The most popular and widely used scheme of magnetic levitation system is controlling a magnetic ball's height above the ground by levitating it against the force of gravity using electromagnets (Khemissi, 2010). These kinds of system are nonlinear, open loop unstable and single-input/single-output (SISO).

Typically, advanced control techniques are applied to control these systems with good performance. Several control methods and approaches are described in literature, like sliding mode control (Khemissi, 2010), (Al-Muthairi and Zribi, 2004), Fuzzy logic control (Choudhary et al, 2012), H_∞ control (Shen, 2002), feedback linearization (Tandon et al., 2014), model reference adaptive control (Torres et al., 2012), LQR (Linear Quadratic Regulator) (Yaseen and Abd, 2017) and LMI (Linear Matrix Inequality) (Khan et al., 2016).

The magnetic levitation system scheme proposed in this work is composed by a Y shape iron plate that must be levitated by the control of electromagnetic forces (Fujii et al., 1994). The system is also nonlinear and open loop unstable. However, this system is multiple-input/multiple-output (MIMO) or multivariable. The inputs are represented by voltages applied to three electromagnets and the outputs are represented by three plate positions. A controller must be designed so that the plate positions track input references with adequate performance. The proposed method to control the system uses Glover-McFarlane H_∞ loop shaping design (Glover and MacFarlane, 1992). This method is a combination of H_∞ robust stabilization with classical loop shaping and presents good performance and robustness when applied to several control problems. For the evaluation of the controller, numerical simulations results were obtained with Matlab/Simulink.

2. SYSTEM MODELING

The schematic diagram of magnetic levitation system is presented in Fig.1 (Fujii et al., 1994). Three electromagnets are mounted above three edges of the Y shape iron plate of mass M and provide attractive forces F_1, F_2, and F_3 for levitation. These attractive forces are controlled by the input voltages u_1, u_2 and u_3 from the controller through the corresponding currents i_1, i_2 and i_3 in the coils. Three gap sensors, mounted below the edges of iron plate, measure the gap lengths or plate positions r_1, r_2 and r_3 between the plate edges and the corresponding electromagnets.

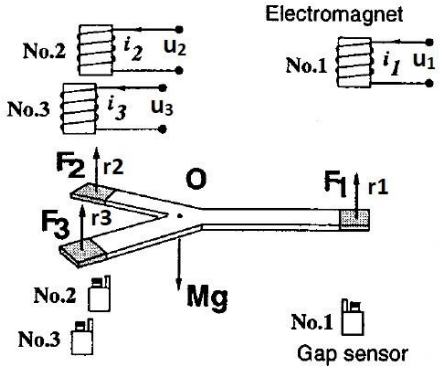

Figure 1. Schematic diagram of magnetic levitation system (Fujii et al., 1994).

The coordinate axes, showed in Fig. 2, are represented by plate gap length at the center of gravity G (x_v), pitching angle (x_p) and rolling angle (x_r). The parameters of iron plate and magnetic levitation system are presented in Fig. 3 and Table 1. M is the total mass of the plate, J_p and J_r are moments of inertia in pitching (x_p) and rolling (x_r) directions, respectively, g is gravitational acceleration, x_v^* is plate gap length at the equilibrium point and u_1^*, u_2^* and u_3^* are the input voltages at the equilibrium point. The symbol * represents the variable value at the equilibrium point. *k1*, *k2* and *k3* are constants related to each electromagnet.

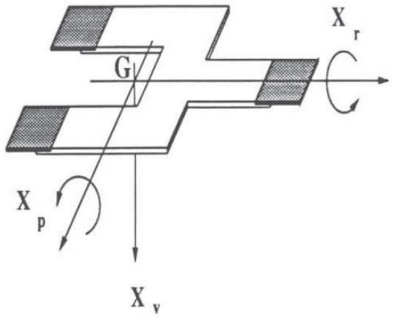

Figure 2. Coordinate axes of magnetic levitation system (Fujii et al., 1994).

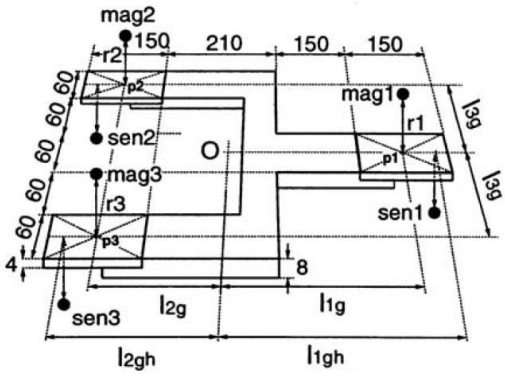

Figure 3. Schematic diagram and parameters of iron plate. *mag*, *sen*, *p* and *O* means electromagnets, gap sensors, acting points of electromagnets forces and the origin of three coordinate axes (Fujii et al., 1994).

Table 1. Parameters values of magnetic levitation system (Fujii et al., 1994).

Unit	Value	Unit	Value	Unit	Value	Unit	Value
l_{1g} [m]	0.327	l_{2gh} [m]	0.218	g [m/s^2]	9.81	u_3^* [V]	3.04
l_{2g} [m]	0.183	M [kg]	1.97	x_v^* [m]	0.018	k_1 [Nm^2/V]	2.42 x 10^{-4}
l_{3g} [m]	0.12	J_p [kgm^2]	5.29 x 10^5	u_1^* [V]	3.17	k_2 [Nm^2/V]	1.93 x 10^{-4}
l_{1gh} [m]	0.362	J_r [kgm^2]	9.35 x 10^4	u_2^* [V]	3.15	k_3 [Nm^2/V]	2.07 x 10^{-4}

Under several idealized assumptions, the equations of vertical, pitching and rotating motions for the magnetic levitation system can be written respectively as (Fujii et al., 1994)

$$M\ddot{x}_v = Mg - (F_1 + F_2 + F_3) \tag{1}$$

$$J_p\ddot{x}_p = F_1 l_{1g} - (F_2 + F_3) l_{2g} \tag{2}$$

$$J_r\ddot{x}_r = (F_2 - F_3) l_{3g} \tag{3}$$

The magnetic attraction forces can be written as a nonlinear function of the input voltages and plate positions:

$$F_j = k_j \left(\frac{u_j}{r_j}\right)^2 \quad j = 1,2,3 \tag{4}$$

The plate positions r_1, r_2 and r_3, are written by

$$r_1 = x_v - l_{1g} tan(x_p) \tag{5}$$

$$r_2 = x_v + l_{2g} tan(x_p) - l_{3g} tan(x_r) \tag{6}$$

$$r_3 = x_v + l_{2g} tan(x_p) + l_{3g} tan(x_r) \tag{7}$$

The system dynamic in state-space is defined as

$$\dot{x} = f(x, u) \tag{8}$$

$$y = g(x, u) \tag{9}$$

where $x = [x_v \ x_p \ x_r \ \dot{x}_v \ \dot{x}_p \ \dot{x}_r]^T = [x_1 \ x_2 \ x_3 \ x_4 \ x_5 \ x_6]^T$ is the state vector, $u = [u_1 \ u_2 \ u_3]^T$ is the input vector and $y = [r_1 \ r_2 \ r_3]^T = [y_1 \ y_2 \ y_3]^T$ is the output vector. The system can be represented as:

$$\begin{bmatrix} \dot{x}_1 \\ \dot{x}_2 \\ \dot{x}_3 \\ \dot{x}_4 \\ \dot{x}_5 \\ \dot{x}_6 \end{bmatrix} = \begin{bmatrix} x_4 \\ x_5 \\ x_6 \\ g - \frac{1}{M}(F_1 + F_2 + F_3) \\ \frac{F_1 l_{1g} - (F_2 + F_3) l_{2g}}{J_p} \\ \frac{(F_2 - F_3) l_{3g}}{J_r} \end{bmatrix} = \begin{bmatrix} f_1 \\ f_2 \\ f_3 \\ f_4 \\ f_5 \\ f_6 \end{bmatrix} \tag{10}$$

$$\begin{bmatrix} y_1 \\ y_2 \\ y_3 \end{bmatrix} = \begin{bmatrix} x_1 - l_{1g} tan(x_2) \\ x_1 + l_{2g} tan(x_2) - l_{3g} tan(x_3) \\ x_1 + l_{2g} tan(x_2) + l_{3g} tan(x_3) \end{bmatrix} = \begin{bmatrix} g_1 \\ g_2 \\ g_3 \end{bmatrix} \tag{11}$$

As can be seen in Eq. (10) and (11), the system in nonlinear. The method proposed to control the system in this work can only be applied in linear systems. Therefore, the system is linearized around the equilibrium point $x^* = [x_v^* \ 0 \ 0 \ 0 \ 0 \ 0]$ and $u^* = [u_1^* \ u_2^* \ u_3^*]$ using Jacobian matrices and becomes

$$\dot{x} = Ax + Bu \tag{12}$$

$$y = Cx + Du \tag{13}$$

where A is the state matrix, B is the input matrix, C is the output matrix and D is the direct transmission matrix (Ogata, 2009). These matrices are given by:

$$A = \begin{bmatrix} \frac{\partial f_1}{\partial x_1} & \cdots & \frac{\partial f_1}{\partial x_6} \\ \vdots & \ddots & \vdots \\ \frac{\partial f_6}{\partial x_1} & \cdots & \frac{\partial f_6}{\partial x_6} \end{bmatrix} \tag{14}$$

$$B = \begin{bmatrix} \frac{\partial f_1}{\partial u_1} & \frac{\partial f_1}{\partial u_2} & \frac{\partial f_1}{\partial u_3} \\ \frac{\partial f_2}{\partial u_1} & \frac{\partial f_2}{\partial u_2} & \frac{\partial f_2}{\partial u_3} \\ & \vdots & \\ \frac{\partial f_6}{\partial u_1} & \frac{\partial f_6}{\partial u_2} & \frac{\partial f_6}{\partial u_3} \end{bmatrix} \tag{15}$$

$$C = \begin{bmatrix} \frac{\partial g_1}{\partial x_1} & \cdots & \frac{\partial g_1}{\partial x_6} \\ \vdots & \ddots & \vdots \\ \frac{\partial g_6}{\partial x_1} & \cdots & \frac{\partial g_6}{\partial x_6} \end{bmatrix} \tag{16}$$

$$D = \begin{bmatrix} \frac{\partial g_1}{\partial u_1} & \frac{\partial g_1}{\partial u_2} & \frac{\partial g_1}{\partial u_3} \\ \frac{\partial g_2}{\partial u_1} & \frac{\partial g_2}{\partial u_2} & \frac{\partial g_2}{\partial u_3} \\ \frac{\partial g_3}{\partial u_1} & \frac{\partial g_3}{\partial u_2} & \frac{\partial g_3}{\partial u_3} \end{bmatrix} \tag{17}$$

3. GLOVER-MCFARLANE H_∞ LOOP SHAPING DESIGN

The proposed method to control the system uses Glover-McFarlane H_∞ loop shaping design and has been applied to a variety of practical control problems successfully (Glover and MacFarlane, 1992). This method is based on H_∞ robust stabilization combined with classical loop shaping (Skogestad and Postlethwaite, 2005). The procedure consists of three steps: loop shaping, robust stabilization and design of the final feedback controller (Glover and MacFarlane, 1992). In loop shaping design, the closed loop performance is specified in terms of requirements on the open loop singular values. Using a pre-compensator W_1 and a post-compensator W_2, the singular values of the nominal plant are shaped to give a desired open loop shape. The nominal plant G and shaping functions W_1 and W_2 are combined to form the shaped plant, $G_s = W_2GW_1$, as shown in Fig. 4.

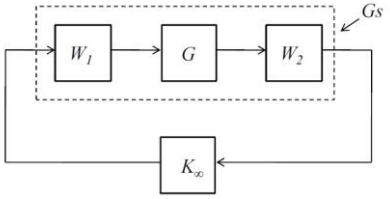

Figure 4. Block diagram of shaped plant G_s (Ban et al., 2009).

The singular values of G_s usually requires high gain at low frequencies, roll-off rates of approximately 20 dB/decade at the desired bandwidth, with higher rates at high frequencies. Some trial and error are involved here. W_2 is usually chosen as a constant, reflecting the relative importance of the output to be controlled and the other measurements being feedback to the controller (Skogestad and Postlethwaite, 2005). This procedure usually guarantees good disturbance attenuation, noise attenuation and robust stability.

In robust stabilization, a controller K_∞ is designed by solving the problem (Ban et al., 2009)

$$\left\| \begin{bmatrix} I \\ K_\infty \end{bmatrix} (I - G_s K_\infty)^{-1} [I \quad G_s] \right\|_\infty < \gamma \tag{18}$$

where $\gamma = \varepsilon^{-1}$ and ε is the robust stability margin. ε is an indicator of the success of the design procedure. It can be shown that if $\varepsilon >= 0.2$, the frequency response of $K_\infty W_2GW_1$ is similar to W_2GW_1 (Glover and MacFarlane, 1992). On the other hand, if ε is too large, the system performance can be deteriorated.

Finally, if is guaranteed that $\varepsilon >= 0.2$, the final feedback controller K is then constructed by combining K_∞ with the shaping functions W_1 e W_2 such that $K = W_2K_\infty W_1$, as shown in Fig. 5.

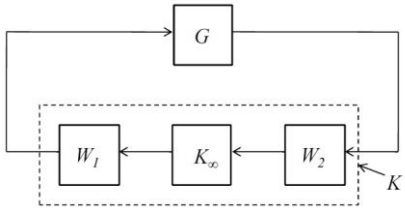

Figure 5. Block diagram of final feedback controller *K* (Ban et al., 2009).

4. SIMULATION RESULT

For the evaluation of controller's performance, robustness and stability, numerical simulations results were obtained with Matlab/Simulink. The system dynamic in state-space was obtained in Eq. (10) and Eq. (11) and linearized around the equilibrium point. The linearized system is represented in Eq. (12) and (13) and the values of matrices *A*, *B*, *C* and *D* are given by:

$$A = \begin{bmatrix} 0 & 0 & 0 & 1 & 0 & 0 \\ 0 & 0 & 0 & 0 & 1 & 0 \\ 0 & 0 & 0 & 0 & 0 & 1 \\ 1089.7 & -16.5 & 0 & 0 & 0 & 0 \\ 0 & 0 & 0 & 0 & 0 & 0 \\ 0 & 0 & 0 & 0 & 0 & 0 \end{bmatrix} \tag{19}$$

$$B = \begin{bmatrix} 0 & 0 & 0 \\ 0 & 0 & 0 \\ 0 & 0 & 0 \\ -2.4038 & -1.9050 & -1.9718 \\ 0 & 0 & 0 \\ 0 & 0 & 0 \end{bmatrix} \tag{20}$$

$$C = \begin{bmatrix} 1 & -0.3270 & 0 & 0 & 0 & 0 \\ 1 & 0.1830 & -0.12 & 0 & 0 & 0 \\ 1 & 0.1830 & 0.12 & 0 & 0 & 0 \end{bmatrix} \tag{21}$$

$$D = \begin{bmatrix} 0 & 0 & 0 \\ 0 & 0 & 0 \\ 0 & 0 & 0 \end{bmatrix} \tag{22}$$

The pre-compensator W_1 and a post-compensator W_2 chosen were

$$W_1 = \begin{bmatrix} \frac{s+10}{0.1s+0.05} & 0 & 0 \\ 0 & \frac{s+10}{0.1s+0.05} & 0 \\ 0 & 0 & \frac{s+10}{0.1s+0.05} \end{bmatrix} \tag{23}$$

$$W_2 = \begin{bmatrix} 1000 & 0 & 0 \\ 0 & 1000 & 0 \\ 0 & 0 & 1000 \end{bmatrix} \tag{24}$$

and the final feedback controller *K* was obtained using Matlab function *ncfsyn* (Gu et al., 2013). It was obtained $\gamma = 3.6181$ and $\varepsilon = 0.2764$. As $\varepsilon >= 0.2$, is expected that the system demonstrates robustness.

The control system implementation in closed loop using Simulink is presented in Fig. 6. The reference inputs are *r1_ref*, *r2_ref* and *r3_ref*, a saturation block was applied to limit the control amplitude (+24 V/-24 V) and disturbance and noise were applied to verify system robustness.

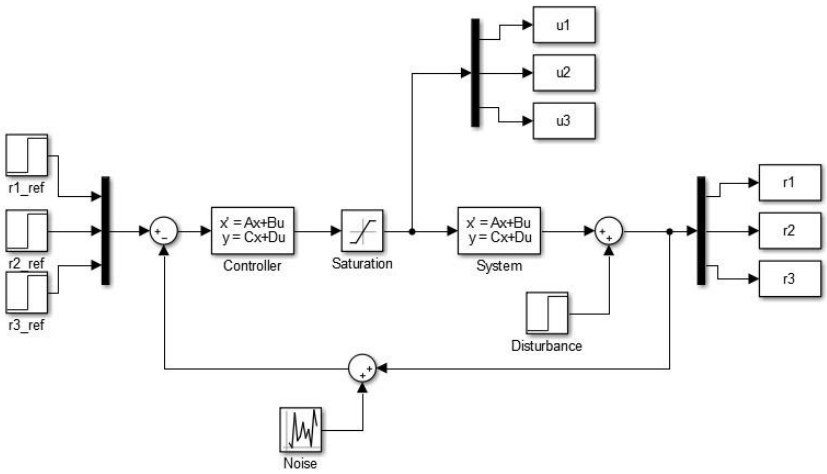

Figure 6. Control system implementation in closed loop using Simulink.

The step response for plate positions r_1, r_2 and r_3 and input voltages u_1, u_2 and u_3, without considering disturbance and noise, are presented in Fig. 7. The step amplitude was 0.01 m and step time 1 s. Analyzing the simulation results, it can be seen that plate positions track the references with good transient and steady state performance and the input voltages present adequate amplitude values for a practical situation.

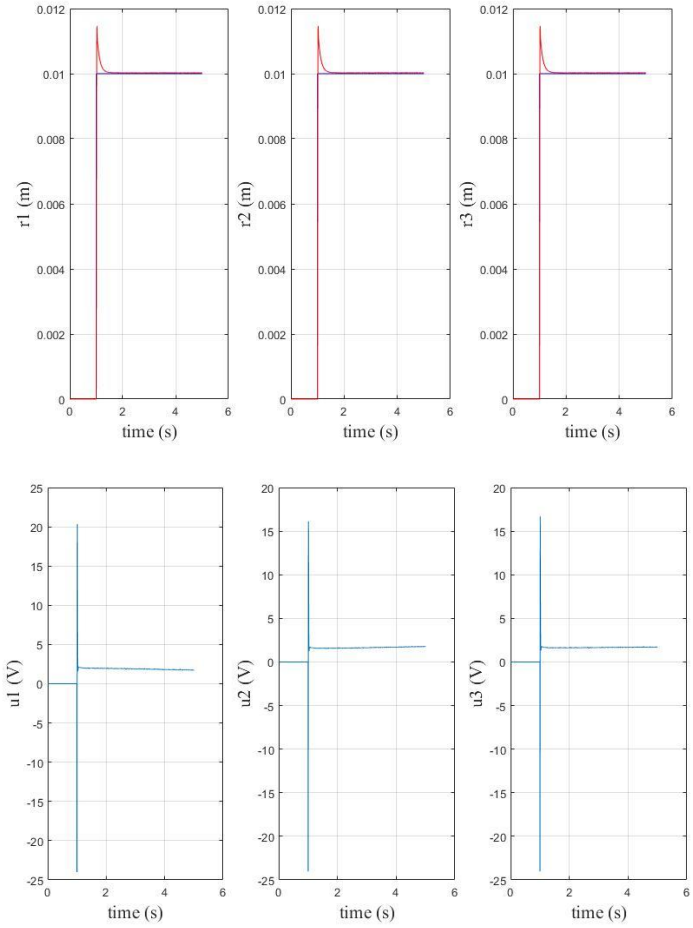

Figure 7. Step responses for the plate positions r_1, r_2 and r_3 (references in blue and plate positions in red) and input voltages u_1, u_2 and u_3 without considering disturbance and noise.

To verify system robustness, it was applied disturbance and noise. The disturbance applied was a step with amplitude 0.001 m and step time 3 s and was considered a random noise uniformly distributed with minimum 0 and maximum

0.0003 m. The step response for plate positions r_1, r_2 and r_3 and input voltages u_1, u_2 and u_3, considering disturbance and noise, are presented in Fig. 8 and Fig. 9, respectively. The noise is presented in Fig. 10. The simulation results demonstrate the system robustness in terms of disturbance and noise attenuation.

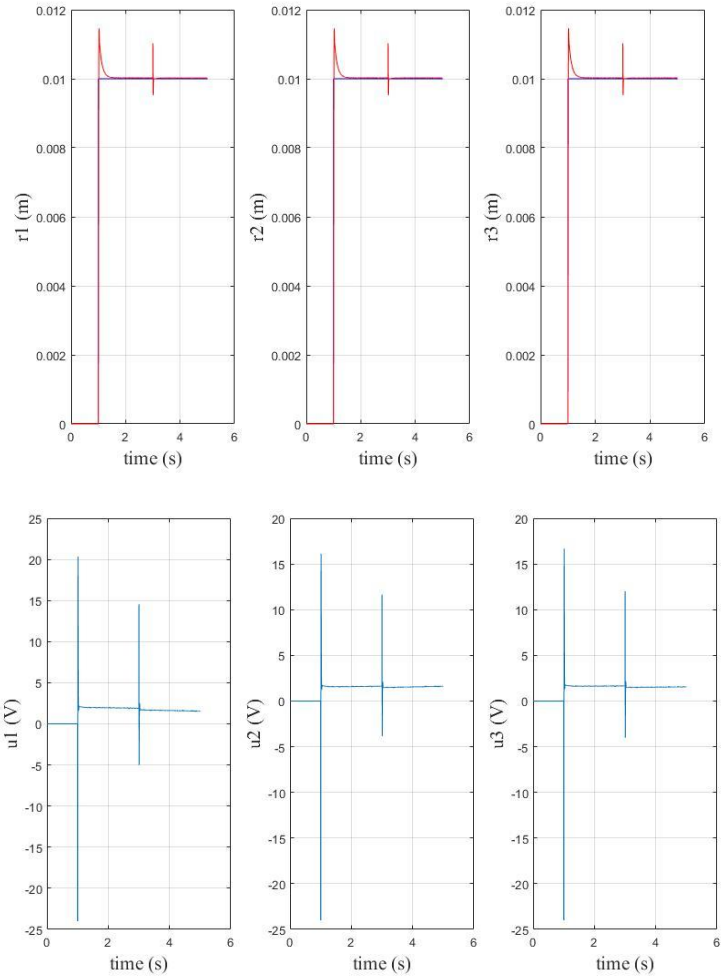

Figure 8. Step responses for the plate positions r_1, r_2 and r_3 (references in blue and plate positions in red) and input voltages u_1, u_2 and u_3 considering disturbance.

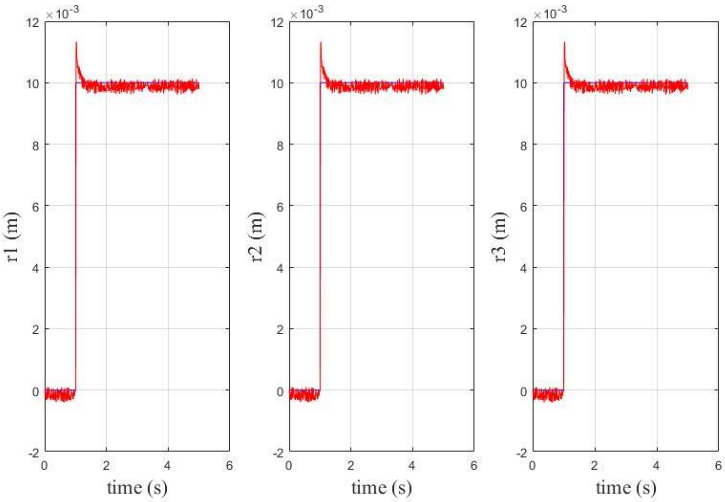

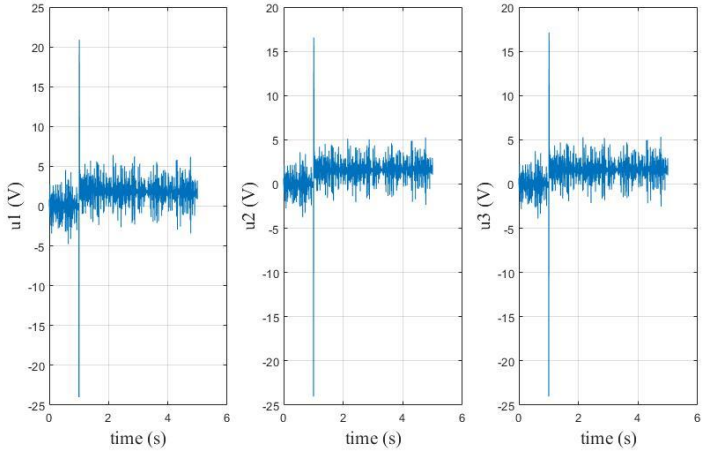

Figure 9. Step responses for the plate positions r_1, r_2 and r_3 (references in blue and plate positions in red) and input voltages u_1, u_2 and u_3 considering noise.

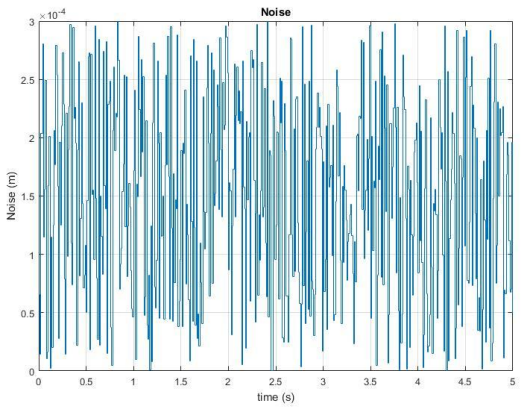

Figure 10. Noise applied in the system.

The robustness was also verified in terms of structured uncertainty in parameters. To realize robust stability analysis, the system is represented in *M-Δ* loop, shown in Fig. 11. *M* represents the control system nominal part and *Δ* represents uncertainty (Skogestad and Postlethwaite, 2005). The robust stability analysis is done by using the structured singular value $\mu_\Delta(M)$. Considering the nominal system *M* stable and $\|\Delta\|_\infty < \beta$, where β is an uncertainty bound, the system of Fig. 11 is robustly stable if and only if $\mu_\Delta(M) \leq 1/\beta$. The structured singular value $\mu_\Delta(M)$ is characterized by upper bound β_u and lower bound β_l. The uncertain system is guaranteed stable for matrices *Δ* with $\|\Delta\|_\infty < \beta_u$ and there exists a specific matrix *Δ* with $\|\Delta\|_\infty = \beta_l$ that destabilizes the system. The robust analysis was realized with Matlab function *robuststab* (Gu et al., 2013). This function calculates the upper bound of stability margin ($1/\beta_l$) and lower bound of stability margin ($1/\beta_u$), decomposing the uncertain system in *M-Δ* loop with $\|\Delta\|_\infty < 1$.

Considering normalized uncertainty $\|\Delta\|_\infty < 1$, it follows that (Gu et al., 2013):

- If $\beta_u < 1$ or $1/\beta_u$ (lower bound of stability margin) >1, the system is robustly stable;
- If $\beta_l > 1$ or $1/\beta_l$ (upper bound of stability margin) <1, the system is not robustly stable;
- If $\beta_l < 1$ or $1/\beta_l > 1$ and $\beta_u > 1$ or $1/\beta_u < 1$, it is not possible to conclude about stability;

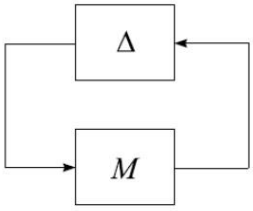

Figure 11. System represented in *M-Δ* loop.

To verify robustness, the parameters M, J_p, J_r, k_1, k_2 and k_3 were changed 15% in relation to the nominal values, shown in Tab. 1. The function *robuststab* reports that uncertain system is robustly stable to modeled uncertainty. This can be seen in Fig. 12, where is presented upper bound (β_u) and lower bound (β_l) of structured singular value as a function of frequency. $\beta_u < 1$ for all frequencies, therefore the system is robustly stable. The step response for plate positions r_1, r_2 and r_3 and input voltages u_1, u_2 and u_3, considering structured uncertainty in parameters, are presented in Fig. 13. The simulation results are very similar to Fig. 7 and demonstrate robustness in terms of parameters variation.

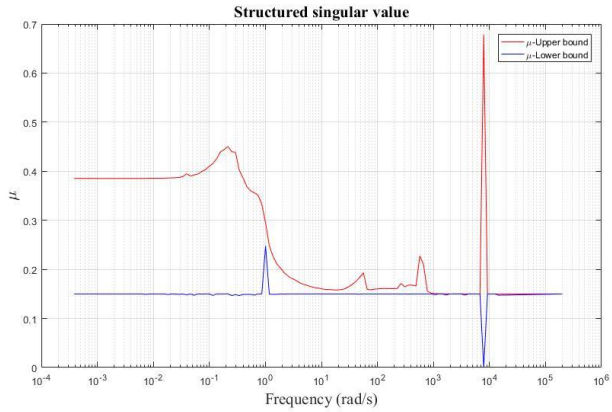

Figure 12. Upper bound (β_u) and lower bound (β_l) of structured singular value as a function of frequency.

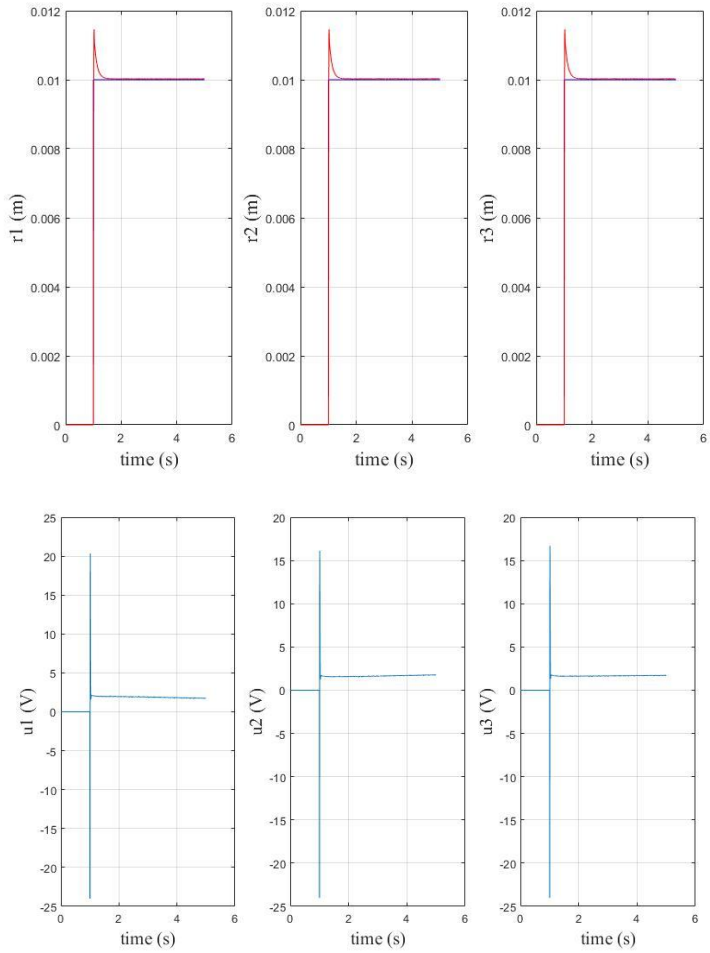

Figure 13. Step responses for the plate positions r_1, r_2 and r_3 (references in blue and plate positions in red) and input voltages u_1, u_2 and u_3 considering structured uncertainty in parameters.

5. CONCLUSIONS

This work describes the control design and implementation for a magnetic levitation system. The proposed method to control the system uses Glover-McFarlane H_∞ loop shaping design. The feedback controller is obtained using Matlab function *ncfsyn*. The pre-compensator W_1 and a post-compensator W_2 chosen ensured that robust stability margin $\varepsilon >= 0.2$. Analyzing the results with Matlab/Simulink, it can be seen that plate positions track the references with good transient and steady state performance and the input voltages present adequate amplitude values for a practical situation. The system demonstrates good performance, stability and robustness when disturbances, noises and parameters variations are applied, as can be seen in step response and structured singular value.

6. ACKNOWLEDGEMENTS

The author acknowledges the support of IFSP (Instituto Federal de São Paulo) – Campus São Paulo.

7. REFERENCES

Al-Muthairi, N.F. and Zribi, M., 2004. "Sliding Mode Control of a Magnetic Levitation System". *Mathematical Problems in Engineering*, Vol. 2004, No. 2, pp. 93–107.

Ban, N., Ogawa, H., Ono, M. and Ishida, Y., 2009. "A Servo Control System Using the Loop Shapimg Design Procedure". *International Journal of Electrical and Computer Engineering*, Vol. 3, No. 12, pp. 2273–2276.

Choudhary, A.K., Nagar, S.K. and Tiwari, J.P., 2012. "Implementation of Fuzzy Controller to Magnetic Levitation System". In *Proceedings of the 9th Control Instrumentation System Conference – CISCON 2012*. Manipal, India.

Fujii, T., Tsujino, T., Suematu, K., Sasaki, K. and Murata, Y., 1994. "Multivariable Control of a Magnetic Levitation System with a Y Shape Iron Plate". *IFAC Advances in Control Education*, Vol. 27, No. 9, pp. 25–28.

Glover, K. and McFarlane, D.C., 1992. "A Loop Shaping Design Procedure Using H_∞ Synthesis". *IEEE Transactions on Automatic Control*, Vol. 37, No. 6, pp. 759-769.

Gu, D.W., Petkov, P.H. and Konstantinov, M.M., 2013. *Robust Control Design With Matlab*. Springer, 2nd edition.

Khan, M., Siddiqui, A.S. and Mahmoud, A.S.A., 2016. "Robust H_∞ Control of Magnetic Levitation System Based on Parallel Distributed Compensator". *Ain Shams Engineering Journal*, Vol. 9, No. 4, pp. 1119–1129.

Khemissi, Y., 2010. "Control Using Sliding Mode of the Magnetic Suspension System". *International Journal of Electrical and Computer Sciences*, Vol. 10, No. 3, pp. 1–5.

Ogata, K., 2009. *Modern Control Engineering*. Prentice Hall, 5th edition.

Shen, J.C., 2002. "H_∞ Control and Sliding Mode Control of Magnetic Levitation System". *Asian Journal of Control*, Vol. 4, No. 3, pp. 333–340.

Skogestad, S. and Postlethwaite, I., 2005. *Multivariable Feedback Control: Analysis and Design*. John Wiley & Sons, 2nd edition.

Tandon, B., Narayan, S. and Kumar, J., 2014. "Explicit Feedback Linearization of Magnetic Levitation System". *International Journal of Electrical and Computer Engineering*, Vol. 8, No. 10, pp. 1870–1874.

Torres, L.H.S., Schnitman, L., Júnior, C.A.V.V and Souza, J.A.M.F., 2012. "Feedback Linearization and Model Reference Adaptive Control of a Magnetic Levitation System". *Studies in Informatics and Control*, Vol. 21, No. 1, pp. 67–74.

Yaseen, M.H.A. and Abd, H.J., 2017. "Modeling and Control for a Magnetic Levitation System Based on SIMLAB Platform in Real Time". *Results in Physics*, Vol. 8, No. 4, pp. 153–159.

8. RESPONSIBILITY NOTICE

The author is the only responsible for the printed material included in this paper.